Experimental investigation of the bonding characteristics and charge distribution of a nitrogen ylide by high resolution X-ray diffraction

Garry T. Smith,[a] **Paul R. Mallinson,***[b] **Christopher S. Frampton**[b] **and Judith A. K. Howard**[a]

[a] *Department of Chemistry, University of Durham, UK DH1 3LE*
[b] *Department of Chemistry, University of Glasgow, UK G12 8QQ*

The experimental charge density of trimethylammonionitramidate, $(CH_3)_3N^+{-}N^-{-}NO_2$, has been determined by high resolution X-ray diffraction. We find the distribution of charge to be more complex than the Lewis formula suggests. Despite the fact that the trimethylammonium fragment bears a full positive charge, the 'onium nitrogen is determined to have a substantial negative charge due to electron donation from the methyl groups by the alkyl inductive effect. The formally negative nitrogen atom of the $N^+{-}N^-$ bond has its charge substantially reduced by the electron-withdrawing nitro group considerably stabilising the molecule. The topological properties of the $-\nabla^2\rho(r)$ distribution for this nitrogen atom suggest it to be sp^2 hybridised.

Introduction

Ylides of first row elements in general contain a quaternary ammonium group bonded to an electronegative atom $[R_3N^+{-}X^-]$. Other than in the case of X = O, the electronegative atom usually requires further stabilisation, achieved by substitution with electron-withdrawing groups to delocalise the formal negative charge. Multiple bonding is not possible due to the full coordination sphere of the quaternary nitrogen atom and the non-availability of nitrogen d orbitals for participation in pπ–dπ bonding, as in the case of the more familiar phosphorus ylide. This unusual $N^+{-}X^-$ bond is of fundamental interest, having both covalent and ionic contributions according to its Lewis formula. Theoretical investigations of such bonds are always limited by computational capabilities, however some excellent studies into the simple model compound $H_3N{-}CH_2$ have been conducted; a study using the generalised valence bond approach[1] gives pictorial evidence for the lack of pπ–dπ bonding in this molecule while a correlated study[2] at the MP2 level using the DZ + d basis set gave a calculated bond length of 1.561 Å, considerably longer than the 1.473 Å calculated for a single bond in $CH_3{-}NH_2$, signifying a weaker bond than expected. In addition, the natural bond order was calculated by the method of Weinhold and co-workers,[3,4] yielding a bond order of only 0.773. Atomic partial charges obtained by the same method give $q_N = -0.795$ and $q_C = -0.741$ signifying that far from the electrostatic contribution across the bond being favourable, it is actually repulsive. It is not too surprising that the formally positive nitrogen atom in fact bears a negative charge; a positive pole is highly electronegative and therefore pulls electron density strongly from its substituents into its own valence shell.

A particular subclass of first-row ylides are the aminimides.[5] In these molecules, the first row atom is also nitrogen giving the general form $R_3N^+{-}N^-{-}Y$. The stabilising Y group is often one which contains a carbonyl group such as Y = CHO, COPh, COMe, CO_2Me, thus allowing the non-bonded density on N^- to be delocalised into the π system as with conventional amides. Such molecules have found utility as carriers for zinc salts through membranes.[6] The weakness of the $N^+{-}N^-$ bond proves industrially useful; thermolytic cleavage of this bond to yield tertiary amines makes aminimides useful polymerization initiators.[7] A further derivative is the case where R and X are part of the same group. Such cyclical aminimides have been investigated by nitrogen NMR[8] and X-ray photoelectron spectroscopy[9,10] where the authors have interpreted their results to be consistent with a displacement of the bonding charge in the $N^+{-}N^-$ bond towards the N^+ atom.

The electron-withdrawing group may take on a different form and in this work we have investigated the electronic properties of trimethylamine nitroimide,[5,11] **1**, where X = NO_2. In this case there are three nitrogen atoms all with different bonding environments and a strong electron-withdrawing group to stabilise the negative charge by delocalisation as shown by the resonance forms. In order to ascertain the characteristics of the $N^+{-}N^-$ bond and the extent of the delocalisation of N^- non-bonding charge in **1**, we have performed an experimental charge density determination by fitting a model which explicitly accounts for the complicated functional form of the electron density to X-ray diffraction data.

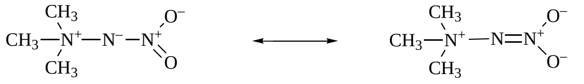

1a **1b**

Experimental

High resolution, single-crystal X-ray diffraction data were measured at low temperature on a CAD4 automated diffractometer as previously described.[12] Data reduction was performed with the DREAM[13] progam suite. The intensities of five standard reflections were measured every 2 h and fitted to cubic polynomials to scale the data for decay correction[13] and the instrument instability factor, *P*, was obtained from the errors in the fit of the polynomials and fluctuations in the standards. An analytical absorption correction was applied by gaussian quadrature on a 16 × 16 × 16 grid using ABSORB.[14] Experimental data are summarised in Table 1. Topological properties of the fitted model of the charge density were obtained with the XDPROP program of the XD package.[15]

Multipole refinement

The crystal structure was determined in earlier work.[5] The backbone of the molecule occupies a mirror plane at $y = \frac{1}{4}$, with two symmetry related CH_3 groups completing the molecule. The multipole refinements were performed using the least-squares part of the XD package.[15] The function $\Sigma w(|F_o| - k|F_c|)^2$ was minimised, where F_o and F_c are the observed

Table 1 Experimental data for trimethylamine nitroimide

Formula	$C_3H_9N_3O_2$
M	119.13
Crystal system	Orthorhombic
Space group	*Pnma*
T/K	123(1)
a/Å	12.064(2)
b/Å	6.622(2)
c/Å	7.051(1)
V/Å^{-3}	563.4(2)
Z	4
D_c/g cm^{-3}	1.405
Crystal dimensions/mm	0.12 × 0.16 × 0.26
μ/cm^{-1}	1.09
Range of corrections for absorption	0.980–0.987
Radiation (λ/Å)	Mo-Kα (0.7107)
Scan type	θ–2θ
$(\sin\theta/\lambda)_{\mathbf{max}}$/Å^{-1}	1.08
Standard reflections	$2\ 3\ \bar{4}$, $6\ 0\ \bar{4}$, $\bar{2}\ 3\ 4$, $0\ 2\ 0$ and $0\ 10\ 0$
No. of reflections measured	13 958
Range *hkl*	−12 to 25; −14 to 14; −15 to 15
No. symmetry-independent reflections	3105
No. $I > 2.5\sigma(I)$ reflections	1732
Agreement factor $R = \Sigma\lvert I - \bar{I}\rvert/\Sigma I$	0.0277
Refined on	F
R	0.0305
R_w	0.0288
S	0.9190
No. variables	133
Weighting scheme, w	$w = \frac{1}{\sigma^2(F)} = \frac{4F^2}{\sigma^2(F^2)}$ $\sigma^2(F^2) = \sigma^2_{\mathrm{counting}}(F^2) + P^2F^4$
P	0.018

and calculated structure factors, respectively, and k is the scale factor which minimises the sum. Only those reflections with $I > 2.5\sigma(I)$ were included in the refinement.

The static charge density is described as a sum of rigid pseudoatoms[16] at the nuclear positions ($\boldsymbol{R}_j$) [eqn. (1)]. Each

$$\rho(\boldsymbol{r}) = \sum_j \rho_j(\boldsymbol{r} - \boldsymbol{R}_j) \qquad (1)$$

pseudoatom density has the form expressed in eqn. (2), where

$$\rho_j(\boldsymbol{r}_j) = P_c\rho_c(\boldsymbol{r}_j) + \kappa'^3 P_v\rho_v(\kappa'^3\boldsymbol{r}_j) + \sum_{l=0}^{l_{\max}} \sum_{m=-l}^{m=+l} \kappa''^3 P_{lm} R_l(\kappa''\boldsymbol{r}_j) d_{lmp}(\theta_j, \varphi_j) \qquad (2)$$

$\boldsymbol{r}_j = \boldsymbol{r} - \boldsymbol{R}_j$. Thus each atom is described by a frozen core of form ρ_c with a fixed population, in our case 2 for C, N and O and spherical valence of the form ρ_v, with the population, P_v, varied in a least squares procedure to allow charge transfer between atoms and the κ' variable allowing for contraction or expansion of the charge cloud of the pseudoatom. Both ρ_c and ρ_v are derived from Clementi and Roetti's Hartree–Fock wavefunctions.[17] The final term in the expansion describes the deviation from sphericity of the valence density by a set of deformation functions taking the shape of density normalised spherical harmonics d_{lmp}. The radial term for these functions is a simple Slater-type function $R_l(\boldsymbol{r}) = Nr^n \exp(-\kappa''\zeta\boldsymbol{r})$ with the expansion–contraction coefficient κ'' again available to improve the radial dependence of the fit. The values of n and ζ are taken from ref. 18, based on orbital product arguments.

An electroneutrality constraint was applied in the refinements. In addition, the crystallographic mirror plane places restrictions[19] on the allowed populations of the spherical harmonics and certain functions were fixed at zero accordingly. A further chemical constraint of identical valence parameters for the two oxygen atoms was introduced.

The level of expansion was truncated at the octapole level ($l_{\max} = 3$) for C, N and O while the asphericity of all H atoms was modelled by a single bond-directed dipole. Both symmetry-independent carbon atoms are expected to have similar environments so they share the same κ' and κ'' values. However, given the disparity in bonding environment of the three nitrogen atoms, they were assigned individual expansion–contraction coefficients. For each atom, the κ'' value was the same for each l value. Each non-hydrogen atom had an anisotropic temperature factor refined while the isotropic temperature factors for the hydrogen atoms were those obtained during conventional, spherical atom refinements using the contracted scattering factor of Stewart *et al.*[20] The C–H bond lengths were subsequently normalised to 1.06 Å, an average value obtained from neutron diffraction experiments.[21] Hydrogen κ' and κ'' were fixed at 1.20 which is equivalent to using the contracted scattering factors.

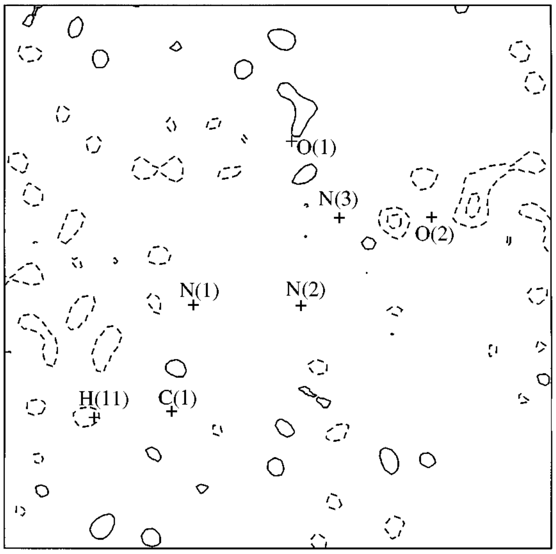

Fig. 1 Residual electron density map in the molecular plane: contour interval = 0.1 eÅ^{-3}; broken lines negative

The refinement resulted in reasonable values for all parameters, however the maximum shift/esd was 0.5 signifying an unconverged refinement. Careful checking of the misfit statistics showed two reflections (5 12 4 and 23 0 2) with F_o an order of magnitude greater than F_c. Removal of these reflections from the refinement allowed convergence to be obtained, improved the agreement statistics and slightly reduced the maximum discrepancies in the residual map. The reason for these rogue reflections could not be ascertained. The in-plane residual map (Fig. 1) shows the disagreement between the data and the model. Only in the region around O(2) is there evidence of discrepancy; various attempts were made to alleviate it, *e.g.* by removing the imposed non-crystallographic symmetry between the two oxygen atoms, none of which was successful. There is no structural residual density anywhere else in the molecule.

A second factor which increases our faith in the fitted model is the result of Hirschfeld's rigid bond test.[22] For atoms of similar masses, it is assumed that there is an effectively vanishing component of the relative vibrational motion of a pair of bonded atoms in the bond direction. If $z^2_{\mathrm{A,B}}$ denotes the mean square displacement amplitude of atom A in the direction of atom B, the difference of amplitudes of a bonded pair of atoms in the bond direction, given in eqn. (3), should tend to zero and

$$\Delta_{\mathrm{A,B}} = z^2_{\mathrm{A,B}} - z^2_{\mathrm{B,A}} \qquad (3)$$

certainly be less than 0.001 Å^2. All bonded pairs easily satisfy this criterion.

Results and discussion

Final agreement factors for the refinement are given in Table 1. A thermal ellipsoid plot is shown in Fig. 2 which also details the

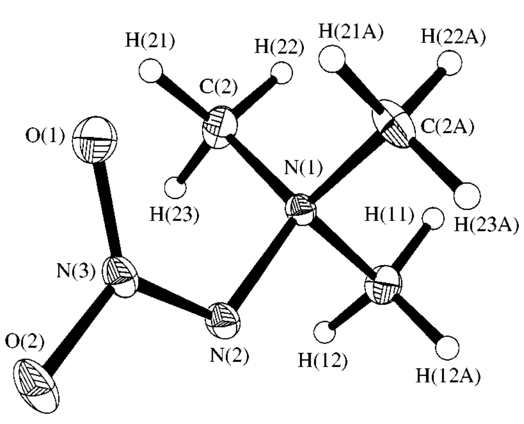

Fig. 2 Thermal ellipsoid plot at the 50% probability level

Table 2 Bond lengths and angles

Bond	Length (this work)/Å	Length (ref. 5)/Å
C(1)–N(1)	1.498(1)	1.490(9)
C(2)–N(1)	1.500(1)	1.507(7)
N(1)–N(2)	1.472(1)	1.470(8)
N(2)–N(3)	1.315(2)	1.323(8)
N(3)–O(1)	1.247(1)	1.265(8)
N(3)–O(2)	1.267(1)	1.252(8)
O(1) · · · H(21)	2.228(1)	2.26(5)
Atoms	Angle (this work)(°)	Angle (ref. 5)(°)
C(1)–N(1)–N(2)	101.9(1)	102.8(5)
C(2)–N(1)–N(2)	113.2(1)	112.4(3)
C(1)–N(1)–C(2)	107.8(1)	107.6(4)
C(2)–N(1)–C(2A)	112.2(1)	113.2(4)
N(1)–N(2)–N(3)	113.6(1)	115.0(5)
N(2)–N(3)–O(1)	125.0(1)	123.0(6)
N(2)–N(3)–O(2)	114.2(1)	115.5(6)
O(1)–N(3)–O(2)	120.9(1)	121.5(6)

Table 3 Experimentally determined monopole populations and κ parameters

Atom	Monopole charge (electrons)	κ'	κ''
C(1)	4.74(8)	0.997(9)	0.72(2)
C(2)	4.53(8)	0.997(9)	0.72(2)
N(1)	5.58(6)	0.964(9)	0.77(4)
N(2)	5.14(8)	0.995(7)	1.08(6)
N(3)	5.2(1)	0.99(1)	0.75(3)
O(1)	6.21(7)	0.998(6)	0.85(6)
O(2)	6.21(7)	0.998(6)	0.85(6)

numbering scheme used. The initial structure determination[5] for this molecule was performed at room temperature and refinements used the independent atom approach. In the current work with high-resolution data and an aspherical atom model, we have observed some small differences in the geometrical parameters. Table 2 contains the bond lengths and angles for non-hydrogen atoms determined here and in the previous study. Of most interest are the lengths of the nitrogen–nitrogen bonds. The N(1)–N(2) bond has length 1.472(1) Å which is comparable to a single covalent bond. The N(2)–N(3) bond however is much shorter at 1.315(2) Å indicating that the resonance form **1b** is a more accurate depiction of the electronic structure.

The electronic charge in a molecule constitutes a single continuous distribution and there exist many schemes for the assignment of 'atomic charges', all of various degrees of rigour. The set of monopole populations of the pseudoatoms from the multipole refinement is one such decomposition and it is reasonable to assume that they provide an appropriate guide to the disposition of charge. The monopole populations for non-hydrogen atoms are shown in Table 3. According to this scheme, the formally positive N(1) has a valence monopole population of 5.58(6) electrons, its substituent carbon atoms are also slightly negatively charged, while all hydrogen atoms are positively charged. This is a manifestation of the alkyl inductive effect. The net valence population of the $(CH_3)_3N^+$ fragment is 25.3(3) electrons compared with the neutral value of 26, indicating that while the nitrogen atom itself does not carry the positive charge as the Lewis structure suggests, this group of the molecule does bear the best part of a full positive charge. Independent evidence that the charge resides on the hydrogen atoms is provided by ^{1}H NMR studies[7,11] on this and similar compounds where the methyl protons have a chemical shift of 3.40 ppm, indicating significant depletion of electron density about their nuclei. The formally fully negatively charged N(2) has a charge of only $-0.14(8)$ while for the NO_2 group this is $-0.62(8)$ showing the extent of electron withdrawal and hence stabilisation of the ylide.

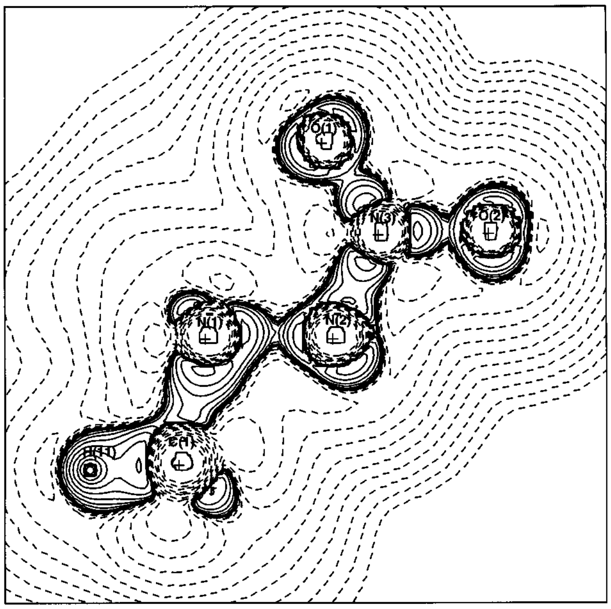

Fig. 3 Experimental Laplacian in the molecular plane

Table 4 Electronic properties at $\rho(\boldsymbol{r}_b)$

Bond	Length/Å	ρ/e Å^{-3}	$\nabla^2\rho$/e Å^{-5}	ε
C(1)–N(1)	1.498(1)	1.64(4)	−9.2(2)	0.45
C(2)–N(1)	1.500(1)	1.68(7)	−13.6(2)	0.32
N(1)–N(2)	1.472(1)	1.90(3)	−2.52(8)	0.01
N(2)–N(3)	1.315(2)	3.34(5)	−30.6(2)	0.53
N(3)–O(1)	1.249(1)	3.82(7)	−25.7(2)	0.32
N(3)–O(2)	1.268(1)	3.46(6)	−21.0(2)	0.33
O(1)· · ·H(21)	2.228(1)	0.12(1)	1.65(1)	0.54

A more informative analysis of the experimental charge density is possible using Bader's *Atoms in Molecules*: *A Quantum Theory*,[23] which is based upon the topological properties of the density $\rho(\boldsymbol{r})$. We have performed such an analysis, in the first instance by searching for the $(3, -1)$ bond critical points (CPs). Any bonded pair of atoms has a bond path, *i.e.* a line of highest electron density linking them. The point on this line where the gradient of $\rho(\boldsymbol{r})$ is zero is termed the bond CP and the properties of the density at this point give quantitative information on that bond's characteristics. Such critical points were located between every atom pair bonded by conventional criteria. In addition, a bond critical point was also located between O(1) and H(21). The values of functions of the density at the bond CPs are listed in Table 4 and a map of the negative Laplacian of the density, $-\nabla^2\rho(\boldsymbol{r})$ is shown for the molecular plane in Fig. 3. The Laplacian of the density, $\nabla^2\rho(\boldsymbol{r})$ contains a large amount of chemical information. Since it is the second derivative of the density, it indicates where density is locally

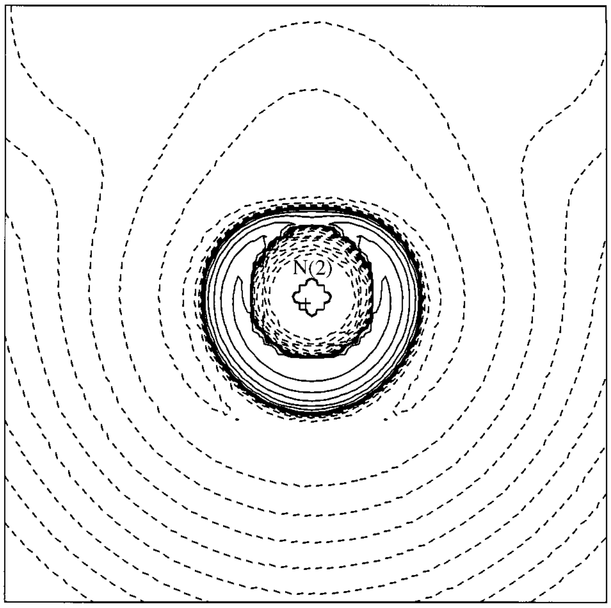

Fig. 4 Experimental Laplacian through N(2) and perpendicular to the molecular plane

concentrated $[\nabla^2\rho(\boldsymbol{r}) < 0]$ and depleted $[\nabla^2\rho(\boldsymbol{r}) > 0]$, and hence graphically shows features such as bonds and lone pairs, which are not observable in $\rho(\boldsymbol{r})$ itself. Solid contours in the Laplacian maps indicate negative Laplacian and hence local concentrations of charge. The contours are on a logarithmic scale.

The values of the density in the C(1)–N(1) and C(2)–N(1) bonds at 1.64(4) and 1.68(7) e Å^{-3} are quite similar and in the range expected, while both bonds show negative Laplacian values indicating a local concentration of charge in the bond and hence covalence. Of note are the unexpectedly high ellipticities of these bonds which may be due to the high degree of polarisation of N(1) which is quite pronounced in the Laplacian map. The N(1)–N(2) bond appears rather pinched here and has $\nabla^2\rho(\boldsymbol{r}_b)$ of a mere −2.52(8) e Å^{-5}, although the density itself is reasonably high at 1.90(3) e Å^{-3}, higher than for the C–N bonds. The ellipticity is not significantly different from zero, indicating no π contribution to the bond. This forces the conclusion that this is a relatively weak bond in agreement with the thermolytic cleavage properties of similar compounds mentioned in the introduction and also the calculated bond order of only 0.773 in the H_3N^+–CH_2^- molecule. In contrast, the N(2)–N(3) bond has a much higher electron density and more negative Laplacian with values of 3.34(5) e Å^{-3} and −30.6(2) e Å^{-5}, respectively, indicating a substantially stronger interaction than a mere single bond and the ellipticity of 0.53 is consistent with a high degree of double bonding character. Of the two resonance forms **1a** and **1b**, one major structural difference in orbital terms is the hybridisation of N(2); for form **1a**, N(2) has sp^3 hybridisation with two σ-bonding and two non-bonding or lone-pair orbitals while for form **1b**, the hybridisation is sp^2 with two σ-bonds, one π-bond and a single sp^2 lone pair. While lone pairs do not show themselves in the total electron density, they do appear as local concentrations of charge in the Laplacian. The Laplacian through N(2) and perpendicular to the molecular plane such that it bisects the expected lone-pair region is shown in Fig. 4. Only one, albeit diffuse, lone pair is observed giving further evidence for resonance form **1b** being more representative of the true structure.

In the original structural report of this compound,[5] the *cis* conformation was attributed to the $N(1)^+\cdots O(1)^{\delta-}$ electrostatic interaction. However, according to the monopole charges, N(1) bears a substantial negative charge and this must bring such a conclusion into question. Also noted in the original work was the existence of a pair of weak hydrogen bonds between O(1) and H(21) and O(1) and H(21A) at 2.26(5) Å. Given that we have shown the positive charge of the amino end of the molecule to reside wholly on the hydrogen atoms, this seems reasonable. All bonds, even weak ones such as these should possess a bond path and (3,−1) CP. This is found to be the case: $\rho(\boldsymbol{r}_b)$ is very low at 0.17(1) e Å^{-3} while the $\nabla^2\rho(\boldsymbol{r}_b)$ is positive at 1.65(1) e Å^{-5}, indicating a closed-shell interaction entirely consistent with a weak hydrogen bond. The Laplacian map in the plane defined by C(2), H(21) and O(1) is shown in Fig. 5. The lone pair of O(1) is approximately aligned with the hydrogen atom.

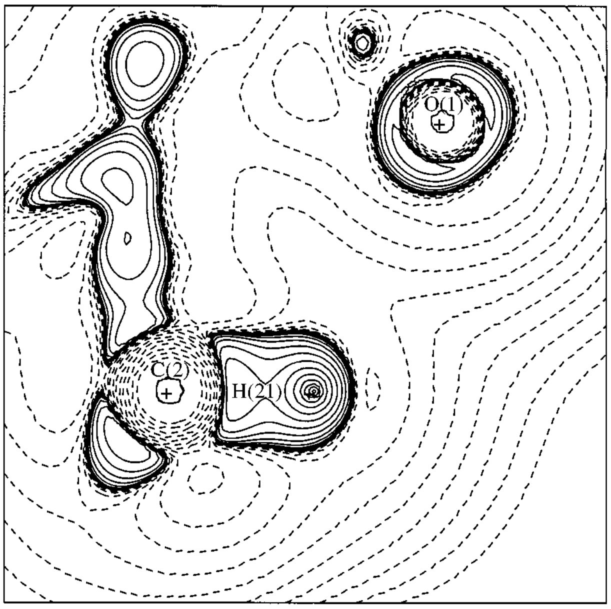

Fig. 5 Experimental Laplacian in the O(1), C(2), H(21) plane showing the O(2)···H(21) interaction

Conclusions

We have investigated the bonding in **1** by analysing the experimentally determined charge distribution, obtained by refining a multipole model against high resolution X-ray diffraction data. We find that the distribution of charge is more subtle than the Lewis formula suggests with the formally positive nitrogen atom bearing a negative charge. The N^+–N^- bond is weaker than a normal single covalent bond while the nitro group delocalises much of the non-bonding charge on N(2), leaving it with only one lone pair. The N(2)–N(3) bond has high double bond character. The original assertion that there exists a hydrogen bond between O(1) and H(21) has been proved correct and this is probably the reason for the *cis* conformation.

Multipole population coefficients are available as supplementary material from the British Library (Suppl. Pub. No. 57521, 2 pp.). Atomic coordinates, thermal parameters, and bond lengths and angles have been deposited at the Cambridge Crystallographic Data Centre (CCDC No. 188/73). For details, see ‘Instructions for Authors’, *J. Chem. Soc., Perkin Trans. 2,* 1997, Issue 1. Any request to the British Library or the CCDC should quote the full literature citation and the relevant reference number.

Acknowledgements

We thank Dr D. G. Morris for a sample of the ylide (**1**), also the EPSRC for support of C. S. F. (GR/F 77852) and a postgraduate studentship for G. T. S.

References

1 D. A. Dixon, T. H. Dunning Jr., R. A. Eades and P. G. Gassman, *J. Am. Chem. Soc.*, 1983, **105**, 7014.

2 T. Naito, S. Nagase, H. Yamataka, *J. Am. Chem. Soc.*, 1994, **116**, 10 080.

3 A. E. Reed, R. B. Weinstock and F. Weinhold, *J. Chem. Phys.*, 1985, **83**, 735.

4 A. E. Reed, L. A. Curtiss and F. Weinhold, *Chem. Rev.*, 1988, **88**, 899.

5 A. F. Cameron, N. J. Hair and D. G. Morris, *J. Chem. Soc., Perkin Trans. 2*, 1972, 1071.

6 S. Tsuchiya and M. Senō, *J. Phys. Chem.*, 1994, **98**, 13 680.

7 S. Inubushi, T. Ikeda and S. Tazuke, *J. Polym. Sci., A*, 1987, **25**, 137.

8 J. Jazwinski, W. Kozminski, L. Stefaniak and G. A. Webb, *J. Mol. Struct.*, 1991, **243**, 365.

9 S. Tsuchiya and M. Senō, *J. Org. Chem.*, 1979, **44**, 2850.

10 S. Tsuchiya and M. Senō, *J. Chem. Soc., Perkin Trans. 2*, 1983, 887.

11 J. Epsztajn and A. R. Katritzky, *Tetrahedron Lett.*, 1969, **54**, 4739.

12 S. T. Howard, M. B. Hursthouse, C. W. Lehmann, P. R. Mallinson and C. S. Frampton, *J. Chem. Phys.*, 1992, **97**, 5616.

13 R. H. Blessing, *J. Appl. Crystallogr.*, 1989, **22**, 396, and references cited therein.

14 G. DeTitta, Program ABSORB, Medical Foundation of Buffalo, USA, 1994.

15 T. Koritsanszky, S. T. Howard, P. R. Mallinson, Z. Su, T. Richter and N. K. Hansen, XD; a computer program package for multipole refinement and analysis of charge densities from diffraction data, 1995.

16 R. F. Stewart, *Acta Crystallogr., Sect. A*, 1976, **32**, 565.

17 E. Clementi and C. Roetti, Atomic Data and Nuclear Data Tables, 1974, **14**, 177.

18 N. K. Hansen and P. Coppens, *Acta Crystallogr., Sect. A*, 1978, **34**, 909.

19 K. Kurki-Suonio, *Israel J. Chem.*, 1977, **16**, 115.

20 R. F. Stewart, E. R. Davidson and W. T. Simpson, *J. Chem. Phys.*, 1965, **42**, 3175.

21 F. H. Allen, O. Kennard, D. G. Watson, L. Brammer, A.G. Orpen and R. Taylor, *J. Chem. Soc., Perkin Trans. 2*, 1987, S1.

22 F. L. Hirshfeld, *Acta Crystallogr., Sect. A*, 1976, **32**, 239.

23 R. F. W. Bader, *Atoms in Molecules: A Quantum Theory*, Oxford University Press, Oxford, 1990.

Paper 6/08234C
Received 6*th December* 1996
Accepted 14*th March* 1997